Fingerprints of entangled spin and orbital physics in itinerant ferromagnets via angle-resolved resonant photoemission

F. Da Pieve

Laboratoire des Solides Irradiés, UMR 7642, CNRS-CEA/DSM, École Polytechnique, F-91128 Palaiseau, France and European Theoretical Spectroscopy Facility (ETSF)

(Received 12 November 2014; revised manuscript received 28 November 2015; published 8 January 2016)

A method for mapping the local spin and orbital nature of the ground state of a system via corresponding flip excitations is proposed based on angle-resolved *resonant* photoemission and related diffraction patterns, obtained here via an *ab initio modified one-step theory* of photoemission. The analysis is done on the paradigmatic weak itinerant ferromagnet bcc Fe, whose magnetism, a correlation phenomenon given by the coexistence of localized moments and itinerant electrons, and the observed non-Fermi-Liquid behavior at extreme conditions both remain unclear. The combined analysis of energy spectra and diffraction patterns offers a mapping of local pure spin-flip, entangled spin-flip–orbital-flip excitations and chiral transitions with vortexlike wave fronts of photoelectrons, depending on the valence orbital symmetry and the direction of the local magnetic moment. Such effects, mediated by the hole polarization, make resonant photoemission a promising tool to perform a full tomography of the local magnetic properties even in itinerant ferromagnets or macroscopically nonmagnetic systems.

DOI: 10.1103/PhysRevB.93.035106

I. INTRODUCTION

Spin and orbital degrees of freedom play a relevant role in many fascinating correlated and/or spin-orbit-driven systems, such as Mott insulators [1–3], nonconventional superconductors [4–6], and topological materials [7–9]. However, in the last two decades, it has become clear that peculiar orbital textures and coupling between spin and orbital degrees of freedom can be found even without relevant spin orbit and/or without relevant electron-electron correlation, as in the case of low-dimensional materials exhibiting Peierls transitions and charge density waves [10–12], some doped lowly correlated insulators developing long-range magnetic order [13], correlated metals [14], and even weak itinerant ferromagnets [15,16], whose behavior might sometimes challenge the standard model of the metallic state, the (ferromagnetic) Fermi-Liquid theory.

Probing simultaneously spin and orbital degrees of freedom with high sensitivity to spatial localization remains however a difficult task. Indeed, the orbital angular momentum is often quenched by the crystal field in many relevant compounds and it does not contribute to the magnetic moment, thus remaining often unaccessible to direct probes with local sensitivity. Also, in many relevant systems, the distinction between incoherent particle-hole and collective modes in both the spin and orbital channels is often not obvious [17,18], making it difficult to understand the role of corresponding fluctuations in collective phenomena. While the commonly used angle-resolved photoemission (ARPES) [19] and resonant inelastic x-ray scattering (RIXS) [20] can give, for certain geometries, information on the angular character of electronic states, their sensitivity to spatial localization is limited due to the linear dependence of the dipole operator on the spatial coordinate $\vec{r}$. The situation becomes even more critical when localized and delocalized electronic states cooperate to determine the properties of a material, like for example in the well investigated weak itinerant ferromagnet bcc Fe. The origin of the ferromagnetism in this system, nowadays seen as a correlation phenomenon given by the coexistence of localized moments associated to electrons in a narrow e_g band and itinerant electrons in the t_{2g} band, is still unclear. A tendency of e_g states to a non-Fermi-Liquid behavior at both extreme PT and ambient conditions has been reported [16] (paramagnetic phase). Unexplained correlations eventually determine the localization of such states [15,21] and the formation of localized moments down to the bcc ferromagnetic phase. Finding a strategy to improve the capabilities of the widely used ARPES and RIXS techniques would boost the advance for an atomic-scale mapping of the magnetic properties of both itinerant ferromagnets and ultimately of disordered or macroscopically nonmagnetic systems.

Orbital-resolved contributions to ARPES spectra are often studied either analyzing the contributions to the self-energy entering the spectral function [22] or analyzing the contributions to circular or linear dichroism in photoemission [23–26], often via the one-step theory. Other more explorative works have considered Auger emission, in particular in time coincidence with photoelectrons, and unraveled the two-hole orbital contributions to both energy spectra [27] and angular polar scans [28,29]. Earlier works have also studied the orbital-resolved contributions to full two-dimensional angular patterns in core level photoemission [30,31] and Auger spectroscopy [32–34], by looking at the anisotropy of the excited "source wave" at the absorber in terms of its l,m components. Recently, pioneering diffraction patterns have also been reported [35–37] for resonant photoemission (RPES), the so called *participator* channel of the nonradiative decay following x-ray absorption. In this channel, the decay occurs before the excited electron has delocalized, leading to one-hole final states linearly dispersing with photon energy (Raman shift) before and at the very edge [38], degenerate with usual ARPES. However, the existing practical calculation schemes (model Hamiltonian-based) [38–41] only focus on the *spectator* channels of the nonradiative decay, with two-holes-like final states, which cannot be reached by direct photoemission. Also, retrieving information on local magnetic properties from RPES (and the Auger-like spectator channels)

remains difficult, and some effects observed in RIXS, such as spin-flip-orbital-flip excitations [18,38,42–45], have never been reported.

In this work, it is shown that the yet largely unexplored spin-polarized *angle-resolved* RPES (AR-RPES) is a promising tool for performing a full *local* spin and orbital tomography of the ground state of a system, by providing access to local spin-flip, orbital-flip, and chiral excitations. The study is based on a recently presented *ab initio modified* one-step theory of photoemission [46,47] for extended systems. Such approach is here reanalyzed to elucidate matrix element effects and mixed with an auxiliary analysis of the partial densities of states to show the connection with local spin and orbital properties. The paradigmatic case of the weak itinerant ferromagnet bcc Fe is considered within density functional theory in the local spin density approximation (DFT-LSDA). The energy spectra and diffraction patterns for excitation at the L_3 edge by circularly polarized light show that (i) exchange transitions induce both pure spin-flip excitations, occurring far from the Fermi level (E_F), and coupled spin-flip–orbital-flip excitations, occurring near E_F in correspondence to a narrow peak in the local partial density of states, associated to the elongated e_g levels; and (ii) the occurrence of such excitations for different experimental geometries depends on the different localization/delocalization of the t_{2g} and e_g states and on the direction of the local moment. The influence of the orbital degrees of freedom in the low energy physics of the system is in line with earlier suggestions about the role of e_g orbitals in the development of local moments [48,49] and with recent combined experimental ARPES and theoretical studies [21]. Similarities and differences with the capabilities of ARPES and RIXS are discussed, as well as relevant implications concerning possible tomographic photoemission experiments for mapping local ground state magnetic properties and low energy excitations in more complex systems.

II. THEORETICAL SECTION

The cross section for resonant photoemission is proportional to the Kramers-Heisenberg formula for second order processes

$$\frac{\partial^2\sigma}{\partial\Omega_p\partial\omega} \propto \sum_f \left| \langle f|D_q|0\rangle + \sum_n \frac{\langle f|V|n\rangle\langle n|D_q|0\rangle}{E_0 - E_n + i\frac{\Gamma_n}{2}} \right|^2 \delta(\hbar\omega + E_0 - E_F)$$

(Γ_n is the core level lifetime-induced width). The first term is the dipole matrix element $D_{vp} = \langle i\epsilon_p L_p\sigma_p|D_q|i\epsilon L_v\sigma_v\rangle$ which describes, in an effective single particle approach, direct valence band photoemission [v (p) denotes the valence state (photoelectron) and $L_p = (l_p,m_p)$]. The second term represents the core excitation and decay, described by the product of the core-absorption dipole matrix elements D_{ck} and the (direct and exchange) Coulomb matrix elements V_d and V_x, i.e., $R_d = V_d \cdot D_{ck} = \langle i\epsilon_p L_p\sigma_p, j'c'|V|i\epsilon L_v\sigma_v, j'\epsilon_k L_k\sigma_k\rangle \cdot D_{ck}$ and $R_x = V_x \cdot D_{ck} = \langle j\epsilon_p L_p\sigma_p, ic'|V|j\epsilon_k L_k\sigma_p, i\epsilon L_v\sigma_v\rangle \cdot D_{ck}$ (k denotes the conduction state where the electron gets excited and c' the quantum numbers m'_c,σ'_c to which the initial hole $c = m_c,\sigma_c$ might scatter). For the more localized participator channel, the direct term describes the process in which the core hole is filled by the excited electron and a valence electron is emitted, while the exchange term describes the process in which these two are exchanged. In principle, the energy detuning from the absorption edge and a narrow bandwidth of the photons can act as a shutter between different channels, although only looking at energy spectra exhibiting the Raman shift (as often done) might not always allow the distinction between localized and delocalized excitations [50]. All delocalized states can be described conveniently via real-space multiple scattering, which describes the propagation of a wave in a solid as repeated scattering events [51] and which allows one to keep explicit dependence on the local quantum numbers. In such basis, the cross section can be cast in a compact form:

$$\frac{\partial^2\sigma}{\partial\Omega_p\partial\omega} = \sum_{qq'} \varepsilon^q \varepsilon^{q'*} \sigma_{qq'},$$

where ε^q are the light polarization tensors and the Hermitian 3×3 matrix $\sigma_{qq'}$ is given by

$$\sigma_{qq'} = \sum_{N,N'} K(N,q)\mathrm{Im}\tau_v(N,N')K^*(N',q'). \qquad (1)$$

$K(N,q)$ are the amplitudes of the overall process (interfering direct and core-hole assisted photoemission) and $\mathrm{Im}\tau_v(N,N')$ is the imaginary part of the scattering matrix for valence states, containing the band structure information of the valence region. N is a label for both the atomic site i and $L = l,m$. The amplitudes can be written as

$$K(iL_v\sigma_v,q) = \sum_{jL_p} B^*_{jL_p}(\mathbf{k_p})\left(\delta_{ij}\delta_{\sigma_v\sigma_p}\left(D_{vp} + R_d\right) + R_x\right)$$

and explicitly contain the photoelectron scattering amplitudes $B_{jL_p}(\mathbf{k_p})$. These can be resumed as $B^*_{jL_p}(\mathbf{k_p}) = Y_{L_p}(\mathbf{k_p})i^{-l_p}e^{i\delta_{l_p}}$, i.e., (the source wave) plus all the scattering contributions. The orbital and spin contributions to the outgoing electron wave function (source wave) are then determined by the parity and Coulomb selection rules of the whole process. They impose that $|l_c - |l_v - l_k|| \leqslant l_p \leqslant l_c + l_v + l_k$, $l_c + l_v + l_k + l_p =$ even, and $m_c + m_p = m_v + m_k$. For the spin, one has $\sigma_c = \sigma_k = \sigma_{c'}$ for the direct term (the spin of the core hole does *not* flip) and $\sigma_c = \sigma_k = \sigma_p$, $\sigma_{c'} = \sigma_v$ for the exchange term (allowing *also* for possible core-hole spin flip leading to simultaneous flip of the orbital projection m_c).

It is important to recall that the anisotropy of the charge density of such source wave and the anisotropy of the charge density of the core-hole state (core-hole polarization, P_c) are influenced by the polarization of the impinging light and the polarization of the valence states. Such anisotropies can be characterized by even multipoles (quadrupole, etc.), describing the alignment (i.e., the deviation from sphericity, given by a different occupation among the different m_l states, with a symmetry between $\pm m_l$), and odd multipoles (dipole, etc.), describing the orientation (i.e., the rotation of the charge density, given by a preferential occupation of m_l states over $-m_l$ states) [52].

The connection with ground state properties is highlighted via an auxiliary description, obtained by modifying an often used expression for normal Auger emission (i.e., a convolution of the density of states for the two final holes [53]). By considering now the density of states (DOS) of the emitted electron $D(E-\epsilon)$ and the DOS of the electron dropping into the core hole $D(\epsilon)$, weighted by the core hole polarization, the intensity becomes

$$I_{\uparrow(\downarrow)}(E) = M_{\uparrow\uparrow(\downarrow\downarrow)}P_{+(-)}\int D_{\uparrow(\downarrow)}(E-\epsilon)D_{\uparrow(\downarrow)}(\epsilon)d\epsilon + M_{\uparrow\downarrow(\downarrow\uparrow)}P_{-(+)}\int D_{\uparrow(\downarrow)}(E-\epsilon)D_{\downarrow(\uparrow)}(\epsilon)d\epsilon,$$

where $P_{\pm} = (1\pm P_c)/2$ takes into account the modifications of the DOS of the electron filling the hole by the core-hole polarization, and $M_{\uparrow\uparrow(\downarrow\downarrow)}$ and $M_{\uparrow\downarrow(\downarrow\uparrow)}$ are, respectively, the sum of the modulus squares of the spin conserving (direct and exchange) decay matrix elements *and* the modulus square of the spin-flip (exchange) decay matrix element:

$$M_{\uparrow\uparrow(\downarrow\downarrow)} = |V_{d,\uparrow\uparrow(\downarrow\downarrow)}|^2 + |V_{x,\uparrow\uparrow(\downarrow\downarrow)}|^2,$$
$$M_{\uparrow\downarrow(\downarrow\uparrow)} = |V_{x,\uparrow\downarrow(\downarrow\uparrow)}|^2.$$

P_c ranges from -1 (as in a ferromagnet with spin down holes, and light impinging parallel to the magnetization [54]) to some other values <1 when the hole flips its spin or the photon polarization and the local valence polarization form a generic angle (in this latter case, both even and odd multipoles contribute to P_c [55], and dichroism occurs in both absorption and decay).

The important theoretical prediction can then be made that the occurrence of spin-flip transitions and their entanglement with orbital ones are determined by the (geometry-dependent) core-hole polarization. Also, orbital flips should be more visible when perturbing a highly symmetric (with respect to relevant quantization axis) intermediate-state orbital population (alignment), rather than an asymmetric one. Given the influence of the core-hole polarization on the weigths of different allowed source waves and the high energy of the photoelectrons (which reduces the importance of final state effects), a selective mapping of local spin and spin-orbital excitations should be possible by looking at two-dimensional angular patterns.

III. COMPUTATIONAL DETAILS

Excitation at the $2p_{3/2}$ edge of the itinerant weak ferromagnet Fe by circularly polarized light is investigated to prove the unique capabilities of AR-RPES. DFT-LSDA potentials obtained by a scalar relativistic linear muffin-tin orbital [56] calculation for the bulk and a semispherical Fe(010) cluster (with 184 atoms and in-plane magnetization along $\langle 001\rangle$) are used as input for a multiple scattering code developed by the author, which can calculate ARPES and AR-RPES from cluster-type objects. Core states are calculated atomically by solving the Dirac equation, while delocalized (bound and unbound) states are developed via multiple scattering. For the optical transitions, the dipole approximation in the acceleration form is used, since the length form is not well defined for the delocalized state. The weak spin-orbit (SO) coupling of the valence and continuum states has been neglected.

From a theoretical viewpoint, nonradiative decays are complicated dynamical processes which include atomic relaxation and electron screening in response to the core hole. However, reasonable approximations can be made for Fe. Electron-core hole interaction is generally weak in metals because of efficient screening of the Coulomb interaction and its only observable effect is the *reduced* branching ratio between the L_3 and L_2 edges of the isotropic x-ray absorption spectra, with respect to what is obtained within the independent particle approximation. However, such reduction is generally smaller for spin-polarized and dichroic spectra, and more importantly, in RPES it only affects the intermediate states, which are not directly observed. For Fe, the deviation of the branching ratio from the statistical value is actually very small [57], indicating a reasonable single particle description. Also, as a consequence of being a weak ferromagnet, both minority and majority spin states can be populated to screen the core hole, leading to no drastic change in the local moment [58]. When the decay takes place, with a valence electron filling the hole and the excited electron emitted, either the effective potential seen by the valence electrons is restored to its initial form or, as the electron is emitted with high kinetic energy, a sudden response of the valence electrons occurs due to the destruction of the core hole, with no time for electrons to readjust. Thus the spin polarization of the emitted electron results in being approximately the one of the intermediate state, very similar to the one of the initial ground state in the case of Fe [59]. Dipole and Auger-like matrix elements are then calculated here using ground state scalar relativistic wave functions. The robustness of the approach is demonstrated by earlier successful comparisons between calculated spin polarization, energy spectra and diffraction patterns and experiments [46,60].

IV. RESULTS

A. AR-RPES spectra and diffraction patterns for parallel geometry

Figures 1(a) and 1(b) show the partial DOS of the *whole* cluster and the ARPES and AR-RPES spectra for a photon energy at the maximum of the resonance for normal emission and parallel geometry (light impinging along the magnetization, along which spin is measured). Each spin-polarized ARPES spectrum shows one main peak and an absence of other sharp features, in agreement with experiments [61] and in line with the genuine lowly correlated nature of the system. The dichroism is null, due to nonchiral geometry and neglected SO in delocalized states. In contrast, the resonant spectra exhibit dichroism (in this geometry only related to the absorption step, as the orientation of the core hole is unaffected by reversal of helicity [62]) and, more importantly, new peaks. Going towards higher binding energies, the spin-up AR-RPES spectra show a first (second) peak for emission from $e_g^{\uparrow}$ ($t_{2g}^{\uparrow}$) states, while the spin-down spectra exhibit a first peak for emission from $t_{2g}^{\downarrow}$ states and then an unexpected peak at an energy where there are almost no spin-down states in the DOS, and which thus corresponds to spin-up valence states. This means that the spin

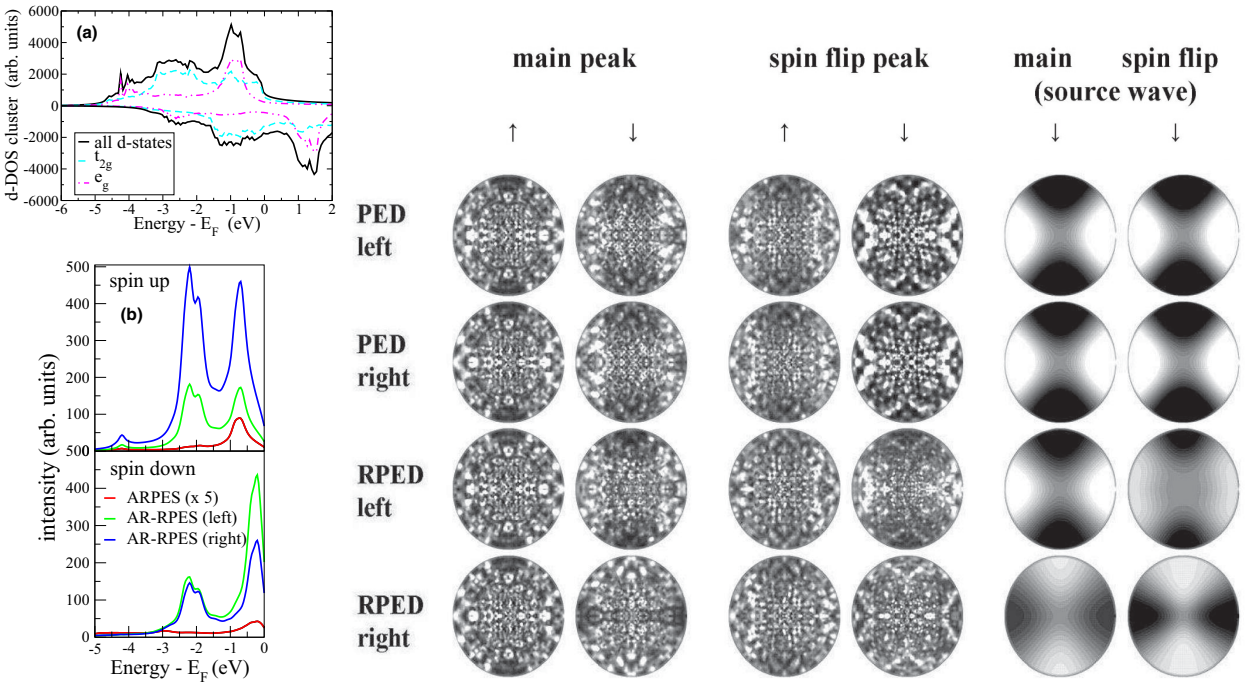

FIG. 1. (a) DOS of the ferromagnetic Fe(010) cluster; (b) ARPES and AR-RPES spectra (from [47]) for parallel geometry and normal emission for excitation at the L_3 edge. Rest of the panel: PED, RPED for initial binding energy corresponding to the main peak and the spin-flip peak in the spin-up AR-RPES spectrum, and "source wave" patterns (the emitter is embedded in the cluster but no scattering events take place). (The plotted function is $\chi = I[\theta,\phi,\epsilon]/I_0[\theta,\epsilon] - 1$, I_0 being the intensity averaged over all ϕ-dependent values. Scans are around the surface normal.)

of the photoelectron is opposite to that of the final valence hole, and thus it is a spin-flip transition. Such (exchange-induced) spin flip can only occur for $2p_{3/2}$ eigenstates with *mixed* spin character due to SO (the $m_j = \pm 1/2$ sublevels, $|3/2,1/2(-1/2)\rangle = \sqrt{2/3}|Y_{10}^{\uparrow}(Y_{10}^{\downarrow})\rangle + \sqrt{1/3}|Y_{11}^{\downarrow}(Y_{1-1}^{\uparrow})\rangle$).

We now move to the more explorative resonant diffraction patterns. *Ab initio* spin-polarized resonant and direct photoemission diffraction patterns (RPED, PED) are reported in Fig. 1, for initial energies corresponding to the two peaks in the *spin-up* AR-RPES spectra (the main peak near E_F and the one at higher binding energy, corresponding to the spin-flip excitations in the spin-down channel). It is clear that, while almost all RPED patterns resemble the corresponding direct ones, a net 90° twist occurs for right circular polarization for the RPED pattern of the spin-down channel, the one allowing for spin-flip transitions, a clear signature of an accompanying *orbital* flip of the photoelectron wave. Interestingly, the effect is actually mainly visible at the main peak, revealing spin-flip transitions hidden by dominating spin-conserving ones in the quasiparticle peak.

This orbital-flip phenomenon can be understood via the two models described in the theoretical section, by analyzing the exchange matrix elements and the local partial DOS. The selection rules dictate $l_p = 1,3,5$ (with 3 numerically found as the most probable wave, in line with previous works on similar transitions [34,63]). Table I reports the exchange transitions occurring at core-hole states with *mixed* spin character (at their spin-down components, as core-hole states will be mainly spin down due to the major availability of spin-down empty states). These are *mixed* spin-flip–orbital-flip transitions, in which both the m_l and σ_z components of the same m_j substate flip. Transitions mixing different m_j states, like $m_j = 1/2$ flipping to $m_j = -1/2$, are also possible, being the m_j sublevels separated by 0.32 eV, but these imply only spin flip. We recall that the relevant irreducible representations here are t_{2g}: $d_{xy} = \frac{1}{\sqrt{2}}(\psi_2 - \psi_{-2})$, $d_{yz} = \frac{1}{\sqrt{2}}(\psi_1 - \psi_{-1})$, $d_{zx} = \frac{1}{\sqrt{2}}(\psi_1 + \psi_{-1})$; e_g: $d_{x^2-y^2} = \frac{1}{\sqrt{2}}(\psi_2 + \psi_{-2})$, $d_{3z^2-r^2} = \psi_0$. Their contribution to the partial DOS around a central absorber ion in the cluster is shown in Fig. 2.

For left-handed light ($\Delta m = +1$ here), the excitation to a $m_k = 1$, $\downarrow$ state ($t_{2g}^{\downarrow}$) (first row in Table I) is more probable than photoexcitation of the other spin-down component of the other sublevel [62]. The numerical evaluation of the decay matrix elements for different orbital contributions, similarly to earlier investigations [58,64,65], allows one to select the dominant

TABLE I. Exchange transitions at core states with mixed spin character, for left (right) polarization $\Delta m = +1$ (-1).

Δm	Edge	$m_c;\sigma_c$	$m_k;\sigma_k$	$m_c';\sigma_c'$	$m_p;\sigma_p$	$m_v;\sigma_v$
+1	$\frac{3}{2};-\frac{1}{2}$	$0;-\frac{1}{2}$	$1;-\frac{1}{2}$	$-1;\frac{1}{2}$	**3**,4,**2**,**1**,0;$-\frac{1}{2}$	**1**,2,**0**,**−1**,−2;$\frac{1}{2}$
+1	$\frac{3}{2};\frac{1}{2}$	$1;-\frac{1}{2}$	$2;-\frac{1}{2}$	$0;\frac{1}{2}$	3,4,2,1,0;$-\frac{1}{2}$	1,2,0,−1,−2;$\frac{1}{2}$
−1	$\frac{3}{2};-\frac{1}{2}$	$0;-\frac{1}{2}$	$-1;-\frac{1}{2}$	$-1;\frac{1}{2}$	**1**,2,**0**,**−1**,−2;$-\frac{1}{2}$	**1**,2,**0**,**−1**,−2;$\frac{1}{2}$
−1	$\frac{3}{2};\frac{1}{2}$	$1;-\frac{1}{2}$	$0;-\frac{1}{2}$	$0;\frac{1}{2}$	**1**,2,**0**,**−1**,−2;$-\frac{1}{2}$	**1**,2,**0**,**−1**,−2;$\frac{1}{2}$

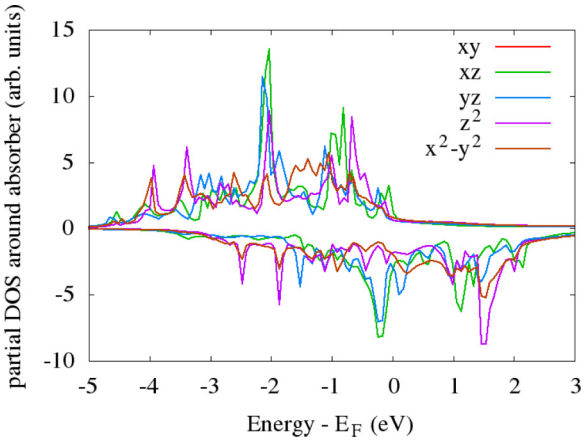

FIG. 2. Local partial DOS (l,m-resolved) around a Fe central ion in the cluster.

transitions (in bold in Table I). Such transitions partially reflect the reasonable result that the decay is more favorable if the two involved valence and conduction electrons have the maximum number of equal quantum numbers, as in this case they will repeal more. The decay leading to a $t_{2g}^{\uparrow}$ final hole with $m_v = \pm 1$ (d_{xz},d_{yz}) gives the strongest contribution, making a distinction between different orbitals in the DOS around the absorber ion (Fig. 2). Indeed, considering the localized nature of the recombination, such DOS unravels the orbital character of the decaying states better than the DOS of the whole cluster, revealing narrow and pronounced peaks from different orbitals of the two irreducible representations in the spin-up main peak. Such narrow peaks remind one of Van Hove singularities in the extended electronic structure [48,66]. Angular momentum conservation rules then dictate a $Y_{33}^{\downarrow}$ emitted wave, with strong intensity reduction along the quantization axis, similarly to the one expected in direct valence band photoemission from a d shell, and in line with previous reports on aligned $f_{\pm 3}$ emitted waves for different compounds [33]. For right-handed light ($\Delta m = -1$), the absorption is equally probable at the two spin-down components of the two mixed spin character sublevels [62]. However, again the numerical evaluation of the product of the matrix elements suggests distinct contributions to the decay, notably a decreasing contribution from the d_{xz} valence states and a stronger one from the $e_g^{\uparrow}$ states with $m_v = 0$ (d_{3z^2-1}). This leads to a $\sim Y_{30}^{\downarrow}$ emitted wave, which is indeed twisted by 90° with respect to the $\sim Y_{3\pm 3}$ behavior expected in usual direct valence band photoemission by left/right polarization. At the spin-flip energy, the effect seems absent, due to a stronger $e_g^{\uparrow}$-$t_{2g}^{\uparrow}$ hybridization and the contribution from more than one orbital of the same irreducible representation (the d_{xz},d_{yz} orbitals of the $t_{2g}^{\uparrow}$). This leads to more balanced contributions of m_l waves and to a petal-like structure.

The results are a demonstration that RPES is sensitive to the very orbital nature of the ground state. Indeed, for elongated orbitals (d_{3z^2-1}) a different type of spin-flip transitions (mixed with an orbital flip) are allowed, contrary to the planar x^2-y^2 and interaxial t_{2g} orbitals. This is similar to what was previously observed in RIXS in cuprates [67]. The phenomenon indeed does remind one of the (local) orbital excitations (local dd excitations) often studied by RIXS via changes in the polarization of the scattered light. Here such excitations manifest themselves as deviations from the anisotropy expected in usual photoemission and can accompany spin-flip satellites in the spectra, even when hidden in the quasiparticle peak. Contrary to ARPES, the photoelectron wave then reflects exactly the orbital character of the valence state, allowing one to map the valence orbital symmetries via monitoring the angular distribution of the resonant current of opposite spin.

Importantly, the spin-flip–orbital-flip excitations involve an $e_g^{\uparrow}$ hole which, being in a completely filled majority spin band, is more localized than those in the partially filled minority spin. These more localized valence flip excitations are then transferred to the photoelectron. The visible orbital-flip effect in the anisotropy of the angular distributions is thus a manifestation of a different correlation in the two bands with different spin, also highlighted by recent experimental and theoretical studies on Auger emission [27], and with different orbital character, as earlier suggested [49]. Orbitals appear quenched far from E_F, where only spin-flip excitations are clear, while spin and orbital degrees of freedom are entangled and both active at low energy in correspondence to a narrow e_g peak near E_F, reminiscent of a Van Hove singularity in the electronic structure [48,66]. The results thus suggest that traces of higher correlation in the relevant e_g band, possibly at the origin of the non-Fermi-Liquid behavior observed at extreme PT [15] and ambient [16] conditions, can be identified even in the phase with long-range magnetic order, often thought of insignificant correlations.

These findings have further fundamental and application-oriented implications. First, despite the local crystal field description used here, the counterpart collective excitations (magnons and orbital waves), occurring in a more complex superexchange scenario, might also be accessed, possibly allowing one to distinguish incoherent particle-hole excitations from collective modes via their dependence on the photon energy [17]. Second, the results show that, at resonance and in a one-step approach, spin-flip transitions might not be accompanied by orbital flip and that, in any case, there is a memory on the photon's polarization. This is contrary to the normal Auger decay, where normally spin-flip transitions are not expected to remember the photon angular momentum (in a two-step process, such transitions should always be balanced by an orbital flip to conserve the total angular momentum, due to the scalar nature of the Coulomb interaction). This suggests that both the Raman shift and the possible memory on the polarization as seen in the angular distributions should be considered when trying to make a distinction between localized and delocalized excitations. Last, an important practical implication is brought by the fact that the flip effect has an atomic nature, as shown by the spin-down source wave patterns (Fig. 1), and disappears for the spin-unpolarized phase (Fig. 3). This demonstrates the sensitivity of RPES to spatial localization, due to the dominance of on-site transitions [46] caused by the $1/r$ behavior of the Coulomb operator, opening the path for elementally sensitive imaging of magnetic domains. Practical implementations might well involve cutting-edge techniques such as spectromicroscopy [68], with energy, angle, and high lateral resolution.

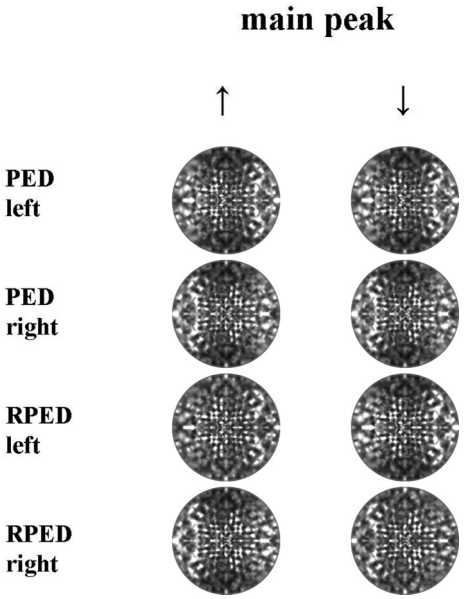

FIG. 3. Spin-polarized PED and RPED patterns for parallel geometry, for excitation at the L_3 edge for paramagnetic Fe(010), and initial state energy corresponding to the main peak in the spin-up channel for the ferromagnetic phase.

B. Diffraction patterns for pependicular geometry

The situation changes drastically when the core-hole polarization changes, i.e., when the photon helicity and the local magnetic moment are oriented differently. Figure 4 reports the patterns for *two different* perpendicular geometries (light impinging perpendicularly to the magnetization), for which the dichroism in absorption is null but the core-hole polarization (now comprising both alignment and orientation)

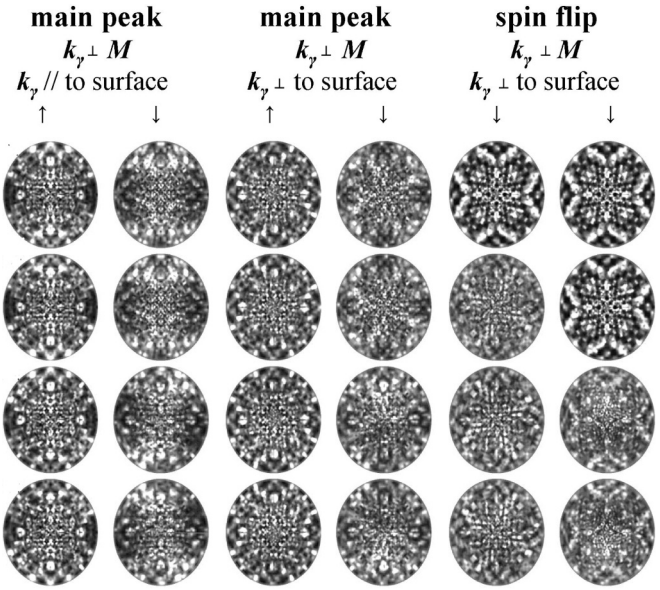

FIG. 4. PED patterns (first two rows, for left and right circular polarization) and RPED patterns (third and fourth rows, for left and right circular polarization) for two perpendicular geometries, for excitation at the L_3 edge for ferromagnetic Fe(010).

does influence differently the emission for left- and right-handed light. As the incident light direction is rotated away from the quantization axis, the selection rules will actually now allow a mixture of $\Delta m = 0, \pm 1$ transitions and thus a detailed microscopic analysis of orbital contributions is more complicated. However, some clear features can be observed.

For grazing incidence (only the main peak energy is considered), the spin-down RPED patterns again deviate from the direct ones, and exhibit a rotation between the two polarizations, though different from the previous 90° flip. Interestingly, when the light is impinging *perpendicularly* to the surface, and thus the scan around the surface normal coincides with a scan around the photon incidence direction, vortexlike features appear for specific channels. Such features are represented by crosses of higher intensity with bending arms following the counterclockwise (clockwise) rotation of the electric field for left- (right-) handed light.

Such effect, called circular dichroism in angular distributions and previously observed in direct photoemission even from nonmagnetic and nonchiral structures [32,69,70], is due to forward scattering peak "rotations" related to the m_l of the emitted wave. It is here unveiled to be correlated with local valence orbital symmetries. Indeed, emission from the t_{2g} (spin-down (-up) emission for the main (spin-flip) peak energy), differentiating from the e_g states by nonisotropic combinations of m_l's, can easily favor nonbalanced combinations with preference towards $\pm m_l$ in the continuum wave, according to the photon's helicity. Chirality in the patterns thus remains, as the emitted wave is now oriented (the asymmetries do not cancel when summing over its m_l components). At the spin-flip energy, the spin-down channel corresponds to emission from mixed e_g-t_{2g} states, and again a petal-like pattern appears. Overall, for these two perpendicular geometries, orbital twists are weakened or absent in the resonant patterns, suggesting smaller contributions of spin-flip terms and a more delocalized valence hole.

V. CONCLUSIONS

In summary, this work presents the exciting prospect of a new generation of resonant photoemission experiments, capable to probe simultaneously the spin polarization, the local valence orbital symmetries, and the orientation of local magnetic moments, exploiting the core-hole polarization as a prism to access spin and orbital excitations.

The results suggest that the analysis of angle-resolved resonant photoemission energy spectra and diffraction patterns can give profound insights into the physics of many fascinating materials. In the case of Fe, orbitals appear quenched far from E_F while a coupling between spin and orbital degrees of freedom is found at lower energy, in correspondence to a narrow peak in the local DOS associated to elongated e_g states. Such coupling should be considered in the development of a unified theory of magnetism including both the localized moment picture and the itinerant electronic behaviour for this system. More generally, the access to different excitations according to the local orbital symmetry would allow one, for example, to probe (metal-oxygen and metal-metal) orbital hybridizations and the competition between electron localization and delocalization in Mott insulators and correlated metals.

From the theoretical point of view, the work suggests that matrix element effects have to be considered in the description of resonant photoemission, which necessarily has to go beyond interpretations based on the sole spectral function or estimations of matrix elements averaged over the full valence region. Last, for the experimental side, the results also challenge the conventional use of RIXS as the main method to probe spin and orbital physics, opening the door for possible explorations of both incoherent particle-hole and collective magnetic excitations also via the nonradiative decay.

ACKNOWLEDGMENTS

The author acknowledges fruitful discussions with P. Krüger at the very early stage of this work, and the financial support from the EU (Marie Curie Fellowship, FP7/2007-2013, Proposal No. 627569).

[1] Y. Tokura and N. Nagaosa, Science **288**, 462 (2000).
[2] K. I. Kugel and D. I. Khomskii, Sov. Phys. JETP **52**, 501 (1981).
[3] W. Brzezicki, J. Dziarmaga, and A. M. Oles, Phys. Rev. Lett. **109**, 237201 (2012).
[4] Z. P. Yin, K. Haule, and G. Kotliar, Nat. Phys. **10**, 845 (2014).
[5] R. B. Laughlin, Phys. Rev. Lett. **112**, 017004 (2014).
[6] V. Aji and C. M. Varma, Phys. Rev. B **75**, 224511 (2007).
[7] W. Witczak-Krempa, G. Chen, Y.-B. Kim, and L. Balents, Annu. Rev. Condens. Matter Phys. **5**, 57 (2014).
[8] H. Zhang, C.-X. Liu, and S.-C. Zhang, Phys. Rev. Lett. **111**, 066801 (2013).
[9] I. Zeljkovic, Y. Okada, C.-Y. Huang *et al.*, Nat. Phys. **10**, 572 (2014).
[10] J. Van Wezel, Europhys. Lett. **96**, 67011 (2011).
[11] T. Ritschel, J. Trinckauf, K. Koepernik, B. Bchner, M. v. Zimmermann, H. Berger, Y. I. Joe, P. Abbamonte, and J. Geck, Nat. Phys. **11**, 328 (2015).
[12] P. A. Bhobe, A. Kumar, M. Taguchi, R. Eguchi, M. Matsunami, Y. Takata, A. K. Nandy, P. Mahadevan, D. D. Sarma, A. Neroni, E. Sasioglu, M. Lezaic, M. Oura, Y. Senba, H. Ohashi, K. Ishizaka, M. Okawa, S. Shin, K. Tamasaku, Y. Kohmura *et al.*, Phys. Rev. X **5**, 041004 (2015).
[13] F. Da Pieve, S. Di Matteo, T. Rangel, M. Giantomassi, D. Lamoen, G.-M. Rignanese, and X. Gonze, Phys. Rev. Lett. **110**, 136402 (2013).
[14] A. Georges, L. de' Medici, and J. Mravlje, Annu. Rev. Condens. Matter Phys. **4**, 137 (2013).
[15] A. A. Katanin, A. I. Poteryaev, A. V. Efremov, A. O. Shorikov, S. L. Skornyakov, M. A. Korotin, and V. I. Anisimov, Phys. Rev. B **81**, 045117 (2010).
[16] L. V. Pourovskii, T. Miyake, S. I. Simak, A. V. Ruban, L. Dubrovinsky, and I. A. Abrikosov, Phys. Rev. B **87**, 115130 (2013).
[17] M. Minola, G. Dellea, H. Gretarsson, Y. Y. Peng, Y. Lu, J. Porras, T. Loew, F. Yakhou, N. B. Brookes, Y. B. Huang, J. Pelliciari, T. Schmitt, G. Ghiringhelli, B. Keimer, L. Braicovich, and M. Le Tacon, Phys. Rev. Lett. **114**, 217003 (2015).
[18] D. Benjamin, I. Klich, and Eugene Demler, Phys. Rev. Lett. **112**, 247002 (2014).
[19] A. Damascelli, Z. Hussain, and Z.-X. Shen, Rev. Mod. Phys. **75**, 473 (2003).
[20] L. J. P. Ament, M. van Veenendaal, T. P. Devereaux, J. P. Hill and J. van den Brink, Rev. Mod. Phys. **83**, 705 (2011).
[21] J. Sánchez-Barriga, J. Fink, V. Boni, I. Di Marco, J. Braun, J. Minar, A. Varykhalov, O. Rader, V. Bellini, F. Manghi, H. Ebert, M. I. Katsnelson, A. I. Lichtenstein, O. Eriksson, W. Eberhardt, and H. A. Dürr, Phys. Rev. Lett. **103**, 267203 (2009).
[22] M. Aichhorn, S. Biermann, T. Miyake, A. Georges, and M. Imada, Phys. Rev. B **82**, 064504 (2010).
[23] C.-Z. Xu, Y. Liu, R. Yukawa, L.-X. Zhang, I. Matsuda, T. Miller, and T.-C. Chiang, Phys. Rev. Lett. **115**, 016801 (2015).
[24] Z.-H. Zhu, C. N. Veenstra, G. Levy, A. Ubaldini, P. Syers, N. P. Butch, J. Paglione, M. W. Haverkort, I. S. Elfimov, and A. Damascelli, Phys. Rev. Lett. **110**, 216401 (2013).
[25] J. Sánchez-Barriga, A. Varykhalov, J. Braun, S.-Y. Xu, N. Alidoust, O. Kornilov, J. Minár, K. Hummer, G. Springholz, G. Bauer, R. Schumann, L. V. Yashina, H. Ebert, M. Z. Hasan, and O. Rader, Phys. Rev. X **4**, 011046 (2014).
[26] C.-H. Park and S. G. Louie, Phys. Rev. Lett. **109**, 097601 (2012).
[27] R. Gotter, G. Fratesi, R. A. Bartynski, F. Da Pieve, F. Offi, A. Ruocco, S. Ugenti, M. I. Trioni, G. P. Brivio, and G. Stefani, Phys. Rev. Lett. **109**, 126401 (2012).
[28] R. Gotter, F. Offi, F. Da Pieve, A. Ruocco, G. Stefani, S. Ugenti, M. I. Trioni *et al.*, J. Electron Spectrosc. Relat. Phenom. **161**, 128 (2007).
[29] F. Da Pieve, D. Sébilleau, S. Di Matteo, R. Gunnella, R. Gotter, A. Ruocco, G. Stefani, and C. R. Natoli, Phys. Rev. B **78**, 035122 (2008).
[30] J. Wider, F. Baumberger, M. Sambi, R. Gotter, A. Verdini, F. Bruno, D. Cvetko, A. Morgante, T. Greber, and J. Osterwalder, Phys. Rev. Lett. **86**, 2337 (2001).
[31] T. Greber and J. Osterwalder, Chem. Phys. Lett. **256**, 653 (1996).
[32] H. Daimon, T. Nakatani, S. Imada, and S. Suga, J. Electron Spectrosc. Relat. Phenom. **76**, 55 (1995).
[33] D. E. Ramaker, H. Yang, and Y. U. Idzerda, J. Electron Spectrosc. Relat. Phenom. **68**, 63 (1994).
[34] T. Greber, J. Osterwalder, D. Naumovic, A. Stuck, S. Hüfner, and L. Schlapbach, Phys. Rev. Lett. **69**, 1947 (1992).
[35] P. Krüger, J. Jupille, S. Bourgeois, B. Domenichini, A. Verdini, L. Floreano, and A. Morgante, Phys. Rev. Lett. **108**, 126803 (2012).
[36] H. Magnan, P. Le Fèvre, D. Chandesris, P. Krüger, S. Bourgeois, B. Domenichini, A. Verdini, L. Floreano, and A. Morgante, Phys. Rev. B **81**, 085121 (2010).
[37] M. Morscher, F. Nolting, T. Brugger, and T. Greber, Phys. Rev. B **84**, 140406(R) (2011).
[38] F. M. F. de Groot, J. Electron Spectrosc. Relat. Phenom. **92**, 207 (1998).
[39] A. Tanaka and T. Jo, J. Phys. Soc. Jpn. **63**, 2788 (1994).
[40] A. Kotani, J. Appl. Phys. **57**, 3632 (1985).
[41] G. Van der Laan and B. T. Thole, J. Phys.: Condens. Matter **7**, 9947 (1995).
[42] L. J. P. Ament, G. Ghiringhelli, M. M. Sala, L. Braicovich and J. van den Brink, Phys. Rev. Lett. **103**, 117003 (2009).

[43] M. van Veenendaal, Phys. Rev. Lett. **96**, 117404 (2006).
[44] F. M. F. de Groot, P. Kuiper, and G. A. Sawatzky, Phys. Rev. B **57**, 14584 (1998).
[45] M. W. Haverkort, Phys. Rev. Lett. **105**, 167404 (2010)
[46] F. Da Pieve and P. Krüger, Phys. Rev. Lett. **110**, 127401 (2013).
[47] F. Da Pieve and P. Krüger, Phys. Rev. B **88**, 115121 (2013).
[48] V. Y. Irkhin *et al.*, J. Phys.: Condens. Matter **5**, 8763 (1993).
[49] J. B. Goodenough, Phys. Rev. **120**, 67 (1960).
[50] P. Glatzel, A. Mirone, S. G. Eeckhout, M. Sikora, and G. Giuli, Phys. Rev. B **77**, 115133 (2008)
[51] D. Sébilleau, R. Gunnella, Z.-Y. Wu, S. Di Matteo, and C. R. Natoli, J. Phys.: Condens. Matter **18**, R175 (2006).
[52] F. Da Pieve, L. Avaldi, R. Camilloni, M. Coreno, G. Turri, A. Ruocco, S. Fritzsche, N. M. Kabachnik and G. Stefani, J. Phys. B **38**, 3619 (2005).
[53] See G. Fratesi, M. I. Trioni, G. P. Brivio, S. Ugenti, E. Perfetto, and M. Cini, Phys. Rev. B **78**, 205111 (2008), and references therein.
[54] B. Sinkovic, E. Shekel, and S. L. Hulbert, Phys. Rev. B **52**, R15703(R) (1995).
[55] F. Da Pieve, S. Fritzsche, G. Stefani, and N. M. Kabachnik, J. Phys. B **40**, 329 (2007).
[56] O. K. Andersen and O. Jepsen, Phys. Rev. Lett. **53**, 2571 (1984).
[57] J. Schwitalla and H. Ebert, Phys. Rev. Lett. **80**, 4586 (1998).
[58] Yu Kucherenko and P. Rennert, J. Phys.: Condens. Matter **9**, 5003 (1997).
[59] T. Wegner, M. Potthoff, and W. Nolting, Acta Phys. Pol. A **97**, 567 (2000).
[60] P. Krüger, F. Da Pieve, and J. Osterwalder, Phys. Rev. B **83**, 115437 (2011).
[61] A. K. See and L. E. Klebanoff, Surf. Sci. **340**, 309 (1995).
[62] G. van der Laan, Appl. Phys. A **65**, 135 (1997). The opposite convention for polarization is used in this work.
[63] L. J. Terminello and J. J. Barton, Science **251**, 1218 (1991).
[64] R. Gotter, F. Da Pieve, F. Offi, A. Ruocco, A. Verdini, H. Yao, R. Bartynski, and G. Stefani, Phys. Rev. B **79**, 075108 (2009).
[65] R. Gotter, F. Offi, A. Ruocco, F. Da Pieve, R. Bartynski, M. Cini, and G. Stefani, Europhys. Lett. **94**, 37008 (2011).
[66] R. Maglic, Phys. Rev. Lett. **31**, 546 (1973).
[67] P. Marra, *Lectures on the Physics of Strongly Correlated Systems XVI: Sixteenth Training Course in the Physics of Strongly Correlated Systems*, AIP Conf. Proc. No. 1485 (AIP, New York, 2012), p. 297.
[68] J. Avila and M. C. Asensio, Synchrotron Radiation News **27**, 24 (2014).
[69] F. Matsui, T. Matsushita, F. Z. Guo, and H. Daimon, Surf. Rev. Lett. **14**, 637 (2007)
[70] N. Mannella, S.-H. Yang, B. S. Mun, F. J. Garcia de Abajo, A. W. Kay, B. C. Sell, M. Watanabe, H. Ohldag, E. Arenholz, A. T. Young, Z. Hussain, M. A. Van Hove, and C. S. Fadley, Phys. Rev. B **74**, 165106 (2006).